Tomographic reconstruction of rainfall maps using attenuation data from cellular networks: the first results based on the Mojette Transform

B. Zohidov*[1], M. Servières[1], N. Normand[2], H. Andrieu[3] J. Langlois[4]

1 CRENAU/IRSTV, Ecole Centrale de Nantes, Nantes, France
2 IRCCYN/IRSTV, Polytech Nantes, Nantes, France
3 IFSTTAR/IRSTV, Nantes, France
4 Ecole Centrale de Nantes, Nantes, France

*Corresponding author: bahtiyor.zohidov@eleves.ec-nantes.fr

Abstract

The real time monitoring of rainfall over urban areas is a critical issue for hydrological applications such as flood warning and water resource systems. Despite the fact that traditional techniques such as networks of rain gauges and weather radars are used to measure rainfall many cities worldwide are not well equipped with these devices. However, they are generally equipped with mobile telecommunication networks. Mobile networks use atmospheric Hyper-Frequency (HF) links whose transmitted signal power is attenuated by rainfall. Measuring that signal attenuation along each link could allow the measurement of path-averaged rainfall. As HF links are concentrated in cities, these networks could constitute a self-sufficient approach to monitoring rainfall.

We propose a simulation approach in order to evaluate the feasibility of reconstruction of rainfall maps by means of tomographic processing applied to attenuation measurements from HF links. A discrete tomographic algorithm based on the Mojette Transform (MT) is applied to reconstruct 2D rainfall map. Before applying the algorithm, specific adjustment procedures, which take into account the geometry of the network topology and non-uniform distribution of links frequency and lengths, are performed. The study domain is the city of Nantes (France) where the density of HF links is greatest. A series of rainfall fields recorded at high spatial (250m x 250m) and temporal (5 minute) resolutions are used to simulate the attenuation data and are considered as reference rainfall fields. These maps are obtained from C-band weather radar located about 10 km north of the center of Nantes (France) and are considered as reference rainfall fields.

We carry out more than 100 reconstruction tests in light rain, shower and storm events to compare the reconstructed rainfall fields to reference ones. Initially obtained results are a subject to further works: (i) improvement on the adjustment procedures of the tomographic reconstruction algorithm, (ii) Implementation of the method in the presence of the error sources.

1. Introduction

The real time monitoring of rainfall is an important issue for urban hydrological applications such as flood warning and water resource management systems. Even though, rain gauges and weather radars are widely used for rainfall measurement, most urban areas worldwide lack such devices. Instead, they are equipped with cellular communication networks. These networks make use of atmospheric Hyper-Frequency (HF) links whose transmitted signal is attenuated by rainfall. The signal attenuation measured along the multiple HF links can be used to retrieve rainfall fields. The retrieval principle is based on the conversion of 1D attenuation vector into 2D rainfall map using well known k-R empirical relation (Olsen, et al., 1978). However, such procedure cannot be directly performed since it is not straightforward and requires a specific inversion technique. The use of tomographic reconstruction algorithms, in this context, is an original approach proposed by (Giuli, et al., 1991) about two decades ago. In the same line of this study, taking advantages of a large number of HF links (Cuccoli, et al., 2011) and (Zinevich, et al., 2008) also applied adaptive

tomographic reconstruction algorithms which process signal attenuation measured along the HF links to retrieve rainfall fields. However, the challenges in the tomographic approach have not been completely explored yet. Therefore, following the same direction as previously cited studies, we evaluate the feasibility of rainfall retrieval using a discrete tomographic technique, which uses the Mojette Filtered Back projection (Guédon & Normand, 2005), applied to attenuation data from HF links in a simulation framework. Section 2 presents how the signal attenuation caused by rain is simulated and the tomographic algorithm used to reconstruct rainfall maps based on the simulated attenuation data. A brief description of the study area and data are given in section 3. The results are detailed in section 4, and conclusion and further works are presented in section 5.

2. Methods

To formulate the problem, the power law model is adopted to relate a signal attenuation to a rain intensity as follows (Olsen, et al., 1978):

$$A = L * aR^b \quad (1)$$

Where, A – total signal attenuation, dB; L – link length, km; R – rain intensity along the link, mm/hour; a and b – power law coefficient which is a function of frequency, polarization, temperature and drop size distribution. In Figure 1b, the network area is represented by n square grids in 2D space (Zinevich, et al., 2008). A rain rate value R_j in the jth pixel is assumed to be constant. Each HF link connects two locations at a distance L_i. We assume that the microwave signal is a straight line travelling through the network area and intersected at a length l_{ij} in the jth pixel:

$$A_i = a_i \sum_{j=1}^{n} l_{ij} R_j^{b_i} + \varepsilon_i, \; i = 1 \ldots m \quad (2)$$

Where, n - number of pixels crossed by the links; R_j – the rain rate in jth pixel, [mm/hour]; l_{ij} - the length of the crossed part of the ith link in jth pixel, [km]; a_i and b_i – the power law coefficients at the ith link frequency and ε_i – measurement error (Atlas & Ulbrich, 1977). As a starting point, we assume that the power law relation is linear and attenuation along the HF link is not influenced by the measurement error. The exponents of power law relations at all frequencies are assumed to be homogenous and linear, that b_i is equal to 1. Then, the eq.(2) will take the following form for m number of links:

$$\begin{bmatrix} A_1 \\ \dots \\ A_m \end{bmatrix} = \begin{bmatrix} a_1 l_{11} & \cdots & a_1 l_{1n} \\ \vdots & \ddots & \vdots \\ a_m l_{m1} & \cdots & a_m l_{mn} \end{bmatrix} \times \begin{bmatrix} R_1 \\ \dots \\ R_n \end{bmatrix} + \begin{bmatrix} \varepsilon_1 \\ \dots \\ \varepsilon_m \end{bmatrix} \quad (3)$$

As a starting point, a total attenuation along the HF link was simulated using eq.(3) in the absence of ε_i. The procedure is applied to 256 real HF links operating at 18, 23 and 38 GHz. The power law coefficients *a, b* are obtained from (ITU-R, 2005).

Tomographic reconstruction algorithm

The objective is to reconstruct rainfall map values $R_1, R_2, \ldots, R_n$ using attenuation data $A_1, A_2, \ldots, A_m$ see eq.(3). The tomographic reconstruction algorithm used to solve the problem is based on the principles of the Mojette Transform (MT) developed by Guédon et al. The MT is a discrete version of Radon Transform. It uses simple linear operations such as addition, subtraction to reconstruct any image from a number of projections (p_i, q_i). A projection value (called a "*bin" as in tomography*) on a projection (p, q) is the sum of pixels value centered on the line as shown in Figure 1:

$$M_R(b,\ p_i,\ q_i) = proj_{p_i,q_i}(b) = \sum_{i=0}^{M-1}\sum_{j=0}^{N-1} R(k,l)\Delta\,(b + q_i * k + p_i * l\,) \quad (4)$$

Where, $R(k,l)$ – a pixel value in (k,l) indices of MxN image; $(p_i,\ q_i)$ - a set of projection direction defined by Farey-Haros series (Servières, et al., 2005); b – a projection value;
Let us consider an example of a 3x3 image in which pixels represent rainfall rate R_1 … R_9, see Figure 1a. The transform domain for the image consists of two projections, namely $p_1,\ q_1 = (1,0)$, $p_2,\ q_2 = (1,1)$. The way of taking projection from the sample image is shown for those two projection directions. Along each projection, bin values are computed by summing up the pixel values in the image. Unlike other tomographic algorithms, the MT has an exceptional property that a number of bins $B(i)$ in each projection depend on the chosen angle ($\theta = \tan\left(\frac{q_i}{p_i}\right)$):

$$B(i) = (M-1)|p_i|\ (N-1)q_i + 1 \quad (5)$$

The Mojette Filtered Back Projection algorithm is applied to reconstruct the rainfall map. However, the algorithm is not directly applicable due to (i) the arbitrary geometry of the network topology, (ii) non-uniform distribution of links frequency and lengths. Therefore, we do specific adjustment procedures before applying the algorithm. In total, the reconstruction process consists of 4 steps including the adjustments:

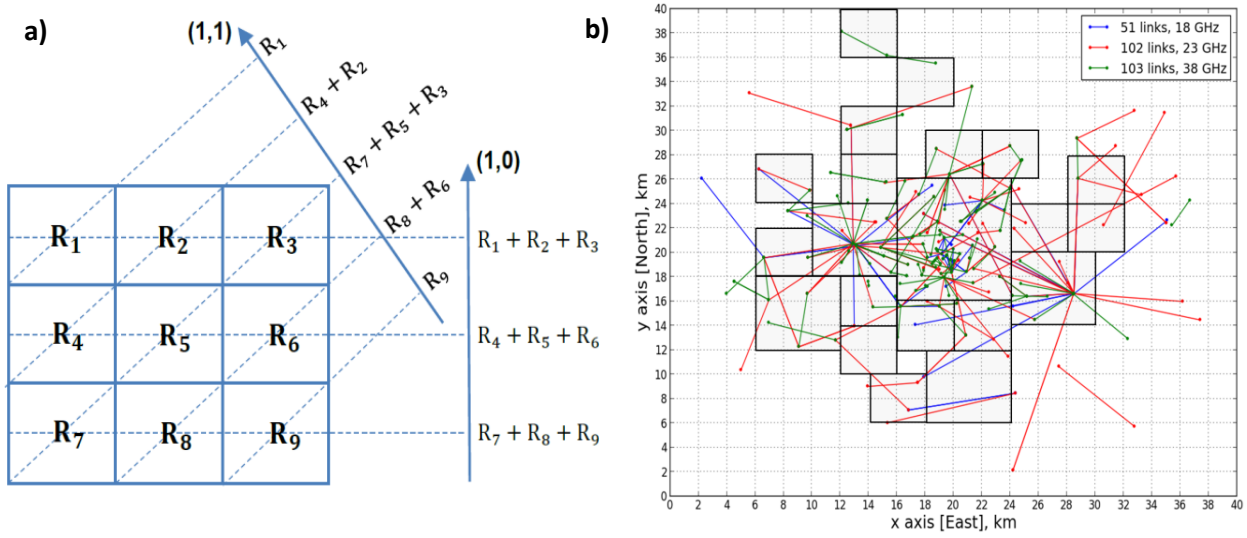

Fig 1: a) An example of Mojette projection at two angles: $(p_1,\ q_1) = (1,0), (p_2,\ q_2) = (1,1)$; b) Microwave links at 18, 23 and 38 GHz in Nantes city. Black rectangles in different sizes illustrate the selected grids for projection and reconstruction of attenuation data.

Step 1. *Grids selection:* The objective is to select valid grids for Mojette projection (acquisition) in the network area. Only zones totally crossed by the HF link are chosen to be reconstructed. We divide the reconstructed zone into sub-grid so that each zone can be reconstructed independently with respect to the attenuation measured through it. In Figure 1b, this is depicted as black rectangles with different area sizes over the study region. In this preliminary study these regions are selected visually.
Step 2. *Projections direction matching:* A set of projections $M_{p,q}$ with discrete Mojette directions are found for the MT acquisition in each grid. We choose discrete (*p, q*) projections directions fitting the best HF link directions and minimizing the number of bins. These possible directions depend on the reconstructed region size. However, only very few bins onto each projection are filled;
Step 3. *Interpolation*: An angular interpolation technique proposed by (Servières, et al., 2006) is applied to fill empty bins in each projection based on nearby values. The interpolation is performed in all selected grids of the network area;

Step 4. *Back Projection*: Mojette Filtered Back Projection algorithm (Guédon & Normand, 2005) is used to reconstruct the attenuation map from the projection values.
These 4 steps are performed in all selected grids of the network. Reconstructed images are assembled, and then normalized with the maximum attenuation value. In the end, the reconstructed map represents a specific attenuation field that could be converted to rainfall map.

Evaluation of the system performance

The reconstructed rainfall map is compared with reference rainfall field using root mean square error (RMSE), which represents the standard deviation of the residuals:

$$RMSE = \sqrt{\frac{1}{n}\sum_{i=1}^{n} (R_i - R_i')^2} \quad (6)$$

Where, R_i – reconstructed rainfall rate; R_i' – reference rainfall rate; n – a length of a rain vector;

3. Data

The study domain is the city of Nantes (France), where the density of HF links is greatest (Figure 1b. We have, at our disposal, hundreds of weather radar images recorded at high spatial (250m x 250m) and temporal (5 minute) resolutions in 7 different periods (Table 1). This C band weather radar of Treillières is located about 10 km north of the center of Nantes. The radar reflectivity images were converted to rain fields with a power law Z-R relation and considered as reference rainfall maps (Emmanuel, et al., 2012).

Table 1. Characteristics of the selected rainfall events.

Rain type	Duration	Number of fields
Light rain	9h 25 min	113
Unorganized storm	2h 50 min	34
Organized storm	2h 50 min	34
Shower	2h 10 min	26

4. Results

To evaluate the monitoring system performance, we carry out a series of rainfall retrieval tests for various rain events such as light rain, shower, organized and unorganized storm. Figure 2 shows a comparison between reconstructed and reference rainfall map by weather radar in a storm event in a linear case with the absence of measurement noise.

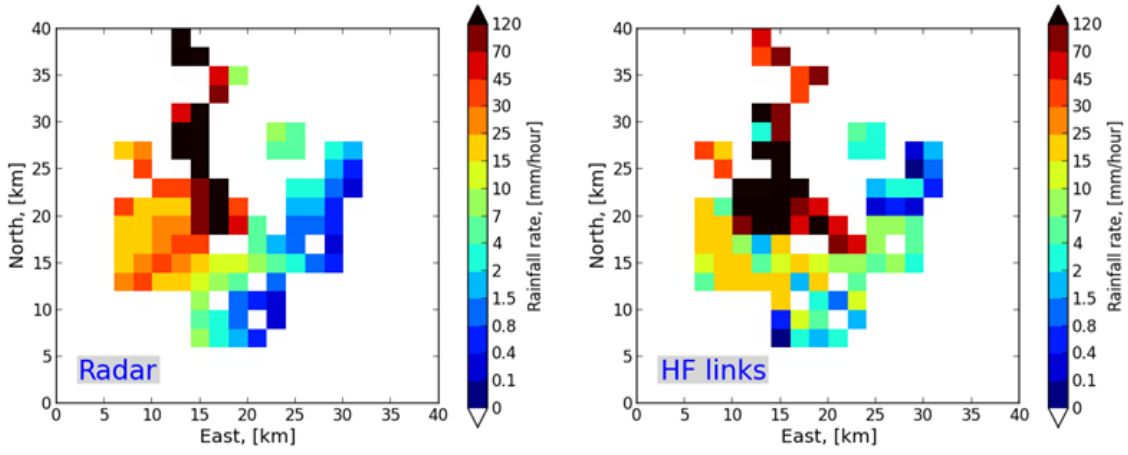

Fig 2: Comparison between reference and reconstructed rainfall maps at 2x2 km2 resolution in storm.

It is worth noting that the MT algorithm was applied to an inhomogeneous network topology for the first time. One can see that the reconstruction by the MT is generally consistent with reference rainfall. The poor performance of the algorithm is due to the following reasons: (i) the accuracy of the MT algorithm strongly depends on a number of projections which are not sufficient along the HF links. In other words, this is called under-determined problem; (ii) the grids choice was manually selected in this study. However, the algorithm is fast enough due to the fact that it uses very simple addition and subtraction operation to reconstruct a rain field.

5. Conclusions

The objective of this paper was to demonstrate the feasibility of rainfall mapping by means of tomographic reconstruction applied to simulated signal attenuation from HF links. Initially obtained results lead to further works in the reconstruction algorithm development part: improvement on a grid selection in step 1, modifying the way of taking projection in step 2, test of other interpolation methods in step 3. Further, the definition of *a priori* knowledge about the state of the problem needs to be addressed since the problem to be solved is highly under-determined in tomography context. A sensitivity analysis to the application conditions, associated error sources in both measurement and reconstruction, spatial and temporal rainfall field structure.

References

Atlas, D. & Ulbrich, C. W., 1977. Path-and area-integrated rainfall measurement by microwave attenuation in the 1-3 cm band. *Journal of Applied Meteorology,* 16(12), pp. 1322-1331.

Cuccoli, F., Facheris, L., Gori, S. & Baldini, L., 2011. *Retrieving rainfall fields through tomographic processing applied to radio base network signals.* s.l., s.n., pp. 81740C--81740C.

Emmanuel, I., Andrieu, H., Leblois, E. & Flahaut, B., 2012. Temporal and spatial variability of rainfall at the urban hydrological scale. *Journal of hydrology,* Volume 430, pp. 162-172.

Giuli, D., Toccafondi, A., Gentili, G. B. & Freni, A., 1991. Tomographic reconstruction of rainfall fields through microwave attenuation measurements. *Journal of Applied Meteorology,* 30(9), pp. 1323-1340.

Guédon, J., 2013. *The Mojette transform: theory and applications.* s.l.:John Wiley \& Sons.

Guédon, J. & Normand, N., 2005. *The Mojette transform: the first ten years.* s.l., s.n., pp. 79-91.

ITU-R, U., 2005. 838-3. Specific attenuation model for rain for use in prediction methods. *Intern. Telecom. Union, Geneva.*

Leijnse, H., Uijlenhoet, R. & Berne, A., 2010. Errors and uncertainties in microwave link rainfall estimation explored using drop size measurements and high-resolution radar data. *Journal of Hydrometeorology,* 11(6), pp. 1330-1344.

Olsen, R. L., Rogers, D. V. & Hodge, D. B., 1978. The aR b relation in the calculation of rain attenuation. *Antennas and Propagation, IEEE Transactions on,* 26(2), pp. 318-329.

Servières, M., Normand, N., Guédon, J., & Bizais, Y. 2005. The Mojette transform: Discrete angles for tomography. *Electronic notes in discrete mathematics*, *20*, 587-606.

Serviéres, M., Normand, N. & Guédon, J.-P., 2006. *Interpolation method for the Mojette transform.* s.l., s.n., pp. 61424I--61424I.

Zinevich, A., Alpert, P. & Messer, H., 2008. Estimation of rainfall fields using commercial microwave communication networks of variable density. *Advances in water resources,* 31(11), pp. 1470-1480.

Zinevich, A., Messer, H. & Alpert, P., 2010. Prediction of rainfall intensity measurement errors using commercial microwave communication links. *Atmospheric Measurement Techniques,* 3(5), pp. 1385-1402.